



HAL
open science

A simple analytical formulation for microbubble drag reduction

Jean-Louis Marié

► **To cite this version:**

Jean-Louis Marié. A simple analytical formulation for microbubble drag reduction. *PhysicoChemical Hydrodynamics*, 1987, 8 (2), pp.213-220. hal-00707879

HAL Id: hal-00707879

<https://hal.science/hal-00707879>

Submitted on 14 Jun 2012

HAL is a multi-disciplinary open access archive for the deposit and dissemination of scientific research documents, whether they are published or not. The documents may come from teaching and research institutions in France or abroad, or from public or private research centers.

L'archive ouverte pluridisciplinaire **HAL**, est destinée au dépôt et à la diffusion de documents scientifiques de niveau recherche, publiés ou non, émanant des établissements d'enseignement et de recherche français ou étrangers, des laboratoires publics ou privés.

A SIMPLE ANALYTICAL FORMULATION FOR MICROBUBBLE DRAG REDUCTION

J. L. MARIÉ

Chargé de Recherche au CNRS, Ecole Centrale de Lyon, Laboratoire de Mécanique des Fluides,
BP 163–69131 Ecully, Cedex France

(Received for publication 29 October 1986)

Abstract—Substantial drag reductions are observed when microbubbles are injected at a surface. A simple analytical formulation for this phenomenon is presented in this paper. It is based on an argument developed by Lumley [*Physics Fluids* 20(10), S64 (1977)]. Following this argument, particles having certain physical properties could affect the turbulence in the buffer layer and thus increase the sublayer thickness with, as a result, a drag reduction. A simple model is derived from this concept and compared to the data obtained by Madavan *et al.* [*J. Fluid Mech.* 156, 237 (1985)] right downstream of the injection section. The agreement is good which tends to prove that this approach is physically meaningful.

1. INTRODUCTION

Evidence of drag reduction due to microbubble injection is given in numerous experiments. A complete survey of the literature has been recently reported [3, 4]. Unfortunately, even in the work of Madavan *et al.* [2], which is very well documented, velocity and turbulence measurements turned out to be impossible because the boundary layers investigated were too thin. For this reason, the physics of such boundary layers remains unknown and the mechanisms of drag reduction very questionable.

According to Legner [3], three effects could be involved in the process: a reduction of the mixture density, an increase of its effective dynamic viscosity and a turbulence modification in the boundary layer. He derives a simple model on these assumptions. The new viscosity is evaluated from the empirical correlation of Sibree [5] and the effect on turbulence is represented by an adequate eddy diffusivity term. He obtains an analytical expression for the decrease of the shear stress, which fits the experimental data of Bogdevich *et al.* [6] quite well.

The increase of the sublayer thickness, as the main mechanism responsible for the decrease of skin friction in polymer and particulate flows, is an idea that was first proposed by Lumley [1, 7]. Madavan *et al.* [8] suggested that the same concept could be used to discuss the action of microbubbles on the wall turbulence. From this remark, they tackled the problem of modeling through a numerical approach [4]. They proposed a phenomenological model in which the influence of the bubbles is simulated by allowing the viscosity and density to vary locally as a function of a prescribed bubble concentration profile. Since the latter profile itself varies downstream with the distance from the injection, it is clear that the mixture can be described by means of a compressible flow analysis. The model is introduced in a numerical code well-tested in compressible boundary layers. A parametric study of the bubble location in the boundary layer, of the peak of concentration and of the viscosity of the mixture is performed. The results of the calculations are of the same order

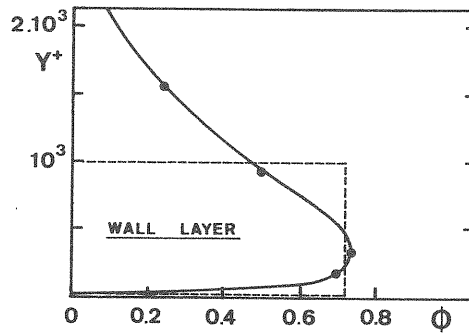


Fig. 1. Typical gas concentration profile in the boundary layer. Line with symbols: measurements of Bogdevich *et al.* [6]. - - - - -: approximate profile.

of magnitude and exhibit the same trends as the experimental drag reduction measurements reported in the literature.

This paper is an attempt to describe the effect of the microbubbles through an analytical form. Due to its simplicity, this formulation could provide useful bases for the development of future sophisticated numerical codes. The size of the bubbles concerned by our approach ranges from 20 to 50 μm . Above this upper limit no more drag reduction is observed [6] and above 1 mm significant increases of the wall shear stress are expected [9]. As in [8], the drag reduction is analysed by assuming that the increase of the sublayer thickness is the main consequence of the action of the bubbles on the turbulence in the buffer layer. This increase is evaluated and the resulting reduction of the friction coefficient is then calculated by a simple analytical relationship. The predictions obtained are quite encouraging.

2. BASIC STATEMENTS

The structure of turbulent boundary layers containing microbubbles is likely to be too complex to allow a general theory to be elaborated. Simplifications are necessary. It is chosen to disregard the influence of certain essential parameters such as the exact shape of the concentration profiles, their streamwise evolution, the effect of buoyancy and of the bubble size. Attention is essentially focused on what happens in a section located immediately downstream of the trailing edge of the porous plate used for microbubble injection, that is, where the drag reduction is maximum. At this location, observations from experiments of various authors [6, 8] exhibit the following facts. The bubble concentration rapidly increases to a maximum (which can sometimes reach 0.6 or 0.8) and then gradually returns to zero in the free-stream. Moreover for reasons still unclear, microbubbles are completely absent in the viscous sublayer. A typical concentration profile drawn from the Soviet measurements [6] is displayed on Fig. 1. For the sake of simplicity, this profile is approximated by a rectangular step distribution with a zero value within the sublayer and a constant maximum value ϕ_m in the wall layer. Similar simplifications were made by Legner [3] and Madavan *et al.* [4]. Denoting by Q_{bubbles} the volumetric concentration of microbubbles and Q_{total} the total volumetric concentration (liquid and bubbles) per unit width of boundary layer, one gets

$$\phi_m = \frac{Q_{\text{bubbles}}}{Q_{\text{total}}}. \quad (1)$$

Now, let us examine how the wall turbulence scales before the microbubbles are injected.

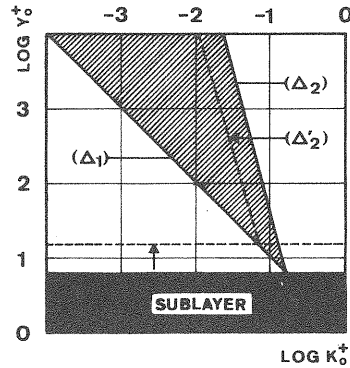


Fig. 2. Scaling relations in the viscous and inertial sublayers, with and without microbubbles. Adapted from [10].

This point has been thoroughly discussed by Lumley [10] in a particularly convincing graphical form. It is briefly recalled here: “In the logarithmic layer there is no relevant length other than Y , the distance from the wall, so that the energy-containing eddies must scale with Y ”. On the energy spectrum, this corresponds to a wave number roughly equal to the inverse of Y , that is $KY = 1$. Denoting by $()_0^+$, the variables non-dimensionalized by U^* (the friction velocity) and ν_0 (the kinematic viscosity of the fluid alone), this equation becomes

$$K_0^+ Y_0^+ = 1 \quad (2)$$

where $Y_0^+ = YU^*/\nu_0$ and $K_0^+ = K\nu_0/U^*$. Besides, the peak of dissipation for Newtonian turbulence is proved to occur at $K_0^+ \eta_0^+ = 0.2$ (see [11]) where η is the Kolmogoroff length scale. A simple scaling analysis from the momentum and kinetic energy equations shows that $\eta_0^+ = (\chi Y_0^+)^{1/4}$ where χ stands for the Karman constant. Thus the equation for the maximum of dissipation reads

$$K_0^+ (\chi Y_0^+)^{1/4} = 0.2 \quad (3)$$

On a logarithmic plot (Fig. 2) equations (2) and (3) appear as two lines Δ_1 and Δ_2 . As quoted by Lumley: “The point where they meet $Y_0^+ = s_0 = 6.35$ marks roughly the outer edge of the viscous sublayer. As a matter of fact, from dynamical considerations, it is known that turbulence can only maintain itself energetically when the scale of the energy-containing eddies is larger than the scale of the dissipative eddies. Since at the point of intersection, the two scales are of the same order, the turbulence becomes essentially dissipative in character and closer to the wall it cannot sustain itself”.

At this level the question is what the action of microbubbles on the turbulence may be. Microbubbles are particles which are approximately three to five times larger than the smallest eddies of the flow, i.e. than the Kolmogoroff’s length scale. As a result, even if the flow field around a microbubble is locally unsteady, the corresponding added mass term should be negligible. Since this term contributes to confer an apparent inertia to microbubbles, the latter can be considered as particles with small inertia. Referring to another study by Lumley [1], we deduce that they likely poorly affect the turbulence by making the dissipation process more efficient, like for certain solid particles. Hence the most probable effect to be expected is both a reduction of the density and an increase of the dynamic viscosity in the region where the microbubbles concentrate, i.e. in the wall layer. From some experimental observations in particle-laden flows [12] it is reasonable to assume that the latter layer still exists with a logarithmic velocity profile which conserves its usual slope. In this perspective

such an alteration of the physical properties will have the following consequences on the diagram in Fig. 2. We assume that the liquid flow rate is adjusted, so that the friction velocity remains constant and equal to its initial value U^* before gas injection. Under these conditions, the sublayer, which is free of bubbles, scales with ν_0 , while the inertial layer, located above, scales with the new kinematic viscosity ν . Thus the two lines Δ_1 and Δ_2 are now given by

$$K^+ Y^+ = 1 \quad (4)$$

$$K^+ (\chi Y^+)^{1/4} = 0.2 \quad (5)$$

which, expressed in terms of the initial viscosity ν_0 , is also equivalent to

$$K_0^+ Y_0^+ = 1 \quad (6)$$

$$K_0^+ (\chi Y_0^+)^{1/4} = 0.2(\nu_0/\nu)^{3/4} \quad (7)$$

ν is larger than ν_0 ; it means that the peak of the energy-containing eddies (line Δ_1 in Fig. 2) remains unchanged whereas the peak of dissipation is translated on the left in Δ_2' . The important result is that the point where the two lines intersect is shifted upward in

$$Y^+ = s = s_0 \frac{\nu}{\nu_0} \quad (8)$$

causing an apparent thickening of the sublayer. In other words, the small eddies of the buffer layer are killed by the increase in kinematic viscosity and so the turbulence is wiped away from the wall. Therefore, the logarithmic profile, whose existence and slope is supposed to be unaffected by the microbubbles, will translate upward, following the equation

$$\frac{U}{U_0^*} = \frac{1}{\chi} \ln Y_0^+ + C \quad (9)$$

where C is larger than the constant C_0 in single-phase flow. The increase $C - C_0$ is easy to relate to the thickening of the sublayer. As a matter of fact s_0 and s are defined as the intersection of the linear velocity distribution and the logarithmic one. Consequently

$$s_0 = \frac{1}{\chi} \ln s_0 + C_0 \quad (10)$$

$$s = \frac{1}{\chi} \ln s + C \quad (11)$$

which yields

$$C - C_0 = s_0 \left(\frac{\nu}{\nu_0} - 1 \right) - \frac{1}{\chi} \ln \frac{\nu}{\nu_0}. \quad (12)$$

However it must be stressed that the value of s_0 derived from equation (10) is greater than 6.35. As a matter of fact, choosing $\chi = 0.41$ and $C_0 = 4.9$ as usual leads to a thickness value of order 10.5. The latter will be used in the next calculations. Let us now examine the implications of this process on the friction coefficient.

3. EVALUATION OF THE DRAG REDUCTION

Attention is focused on the fact that all the calculations in this section are performed at constant U^* . The friction laws without and with microbubbles are respectively written as

$$\frac{U_0^\infty}{U^*} = \left(\frac{2}{CF_0} \right)^{1/2} = \frac{1}{\chi} \ln \frac{U^* \delta_0}{\nu_0} + C_0 + \frac{2\Pi_0}{\chi} \quad (13)$$

$$\frac{U^\infty}{U^*} = \left(\frac{2}{CF} \right)^{1/2} = \frac{1}{\chi} \ln \frac{U^* \delta}{\nu} + C + \frac{2\Pi_0}{\chi} \quad (14)$$

where $2\Pi_0/\chi$ is the wake function introduced by Coles [13] and δ the boundary layer thickness. It implies that microbubbles, unlike larger bubbles [9], do not have any effect on the wake component of the velocity profile which is an admissible hypothesis, referring to the literature concerned with particle-laden flows [14]. In order to simplify, δ is supposed to be only slightly different from δ_0 . It leads to

$$\left(\frac{2}{CF} \right)^{1/2} - \left(\frac{2}{CF_0} \right)^{1/2} = C - C_0 \quad (15)$$

$C - C_0$ is known from equation (12). Thus

$$\left(\frac{CF}{CF_0} \right) U_{\text{const}}^* = \left[1 + \left(\frac{CF_0}{2} \right)^{1/2} \left(10.5 \left(\frac{\nu}{\nu_0} - 1 \right) - \frac{1}{\chi} \ln \frac{\nu}{\nu_0} \right) \right]^{-2}. \quad (16)$$

The problem now consists in modeling the action of the microbubbles on ν . The density of the mixture in the wall layer is defined as

$$\rho = \rho_0(1 - \phi_m) + \rho_G \phi_m \quad (17)$$

where ρ_G is the gas density. Since $\rho_G \ll \rho_0$, the effective density can be approximated by

$$\rho \sim \rho_0(1 - \phi_m). \quad (18)$$

Concerning the dynamic viscosity, several solutions are possible. Because of their small size, microbubbles behave as rigid spheres. That is, their interface is perfectly spherical and undeformable. For a dilute suspension of such particles, Einstein [15] proved that its effective viscosity could be successfully estimated by

$$\mu = \mu_0(1 + 2.5\phi). \quad (19)$$

Since this relationship was derived in the case of negligible particle interactions it is not expected to be well adapted to the present situation. This is why the formulation of Batchelor and Green [16] can be *a priori* preferred. The latter formulation applies to rigid spherical particles of uniform size interacting in a statistically homogeneous suspension. Practically, it is an extension of equation (19) with an additional term of order ϕ^2 , whose coefficient is calculated from theoretical considerations. This coefficient is a function of various parameters of the flow field. In particular, it depends on the probability density for the vector \mathbf{r} separating the centres of two adjacent particles. Due to the turbulent mixing existing in microbubble layers, a density uniform in all the directions seems to be an assumption physically acceptable. Then

$$\mu = \mu_0(1 + 2.5\phi + 5.2\phi^2). \quad (20)$$

Equation (20) was derived for a monodisperse suspension. This is why it should be valid in principle for low gas concentrations. Nevertheless, one will see in what follows, that it works quite well at higher concentrations. In addition, for very small particles, for which the Peclet number is small, the Brownian motion may also give a contribution to the viscosity (Batchelor [17]). Therefore, this effect should be taken into account here. However, for a uniform probability density, the coefficient of ϕ^2 is shown to be 6.2 ([17]), when

Brownian motion is considered. This is a minor correction, which appears as an excessive refinement, regarding the simplicity of our approach. Consequently it is neglected. The expressions of ν associated with the two previous viscosity models are respectively

$$\nu = \nu_0 \frac{1 + 2.5\phi_m}{1 - \phi_m} \quad (21)$$

$$\nu = \nu_0 \frac{1 + 2.5\phi_m + 5.2\phi_m^2}{1 - \phi_m}. \quad (22)$$

In most experiments (see for example [2] or [8]) ratio CF/CF_0 is measured in keeping constant the liquid velocity at infinity. So, in order to make a comparison between the theory and these measurements, equation (16) must be corrected. For that purpose the following argument is used. For a single-phase turbulent boundary layer developing on a smooth flat plate the friction law is given by the well known formula [18]

$$\frac{CF_0}{2} = \frac{U_0^{*2}}{U_0^{\infty 2}} = 0.0296 \left(\frac{U_0^{\infty} X}{\nu_0} \right)^{-1/5} \quad (23)$$

where X is the downstream distance. From the above and by analogy with (23) the friction law in presence of microbubbles can be expected to be of the form

$$\frac{CF}{2} = \frac{U^{*2}}{U^{\infty 2}} = \mathcal{F} \left(\left(\frac{CF_0}{2} \right)^{1/2}, \phi_m \right) \left(\frac{U^{\infty} X}{\nu} \right)^{-1/5}. \quad (24)$$

This being accepted, the ratio of CF to CF_0 at constant U^* reads

$$\left(\frac{CF}{CF_0} \right)_{U^* \text{ const}} = \frac{\mathcal{F}}{0.0296} \left(\frac{U^{\infty}}{U_0^{\infty}} \right)^{-1/5}. \quad (25)$$

Now U^{∞}/U_0^{∞} in the left hand side of (25) is nothing else but $(CF_0/CF)_{U^* \text{ const}}^{1/2}$ so that finally

$$\left(\frac{CF}{CF_0} \right)_{U^* \text{ const}}^{9/10} = \frac{\mathcal{F}}{0.0296}. \quad (26)$$

In the same way, this ratio taken at U^{∞} constant is equal to

$$\left(\frac{CF}{CF_0} \right)_{U^{\infty} \text{ const}} = \frac{\mathcal{F}}{0.0296}. \quad (27)$$

We conclude that the relationship between the two ratios is

$$\left(\frac{CF}{CF_0} \right)_{U^{\infty} \text{ const}} = \left(\frac{CF}{CF_0} \right)_{U^* \text{ const}}^{9/10} \quad (28)$$

and hence

$$\left(\frac{CF}{CF_0} \right)_{U^{\infty} \text{ const}} = \left[1 + \left(\frac{CF_0}{2} \right)^{1/2} \left(10.5 \left(\frac{\nu}{\nu_0} - 1 \right) - \frac{1}{\chi} \ln \frac{\nu}{\nu_0} \right) \right]^{-9/5}. \quad (29)$$

Equation (29) is compared with the measurements of Madavan *et al.* [2]. The data selected for the comparison were obtained from a flush mounted hot film located at 51 mm downstream the injection section. No investigation was performed closer to this section, even in the other experiments of the literature. Moreover these data correspond to the situation where the plate is above the boundary layer. Thus the migration of the microbubbles

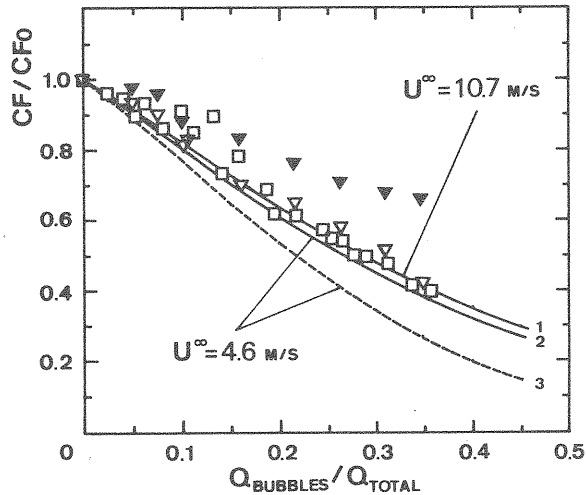


Fig. 3. Effect of microbubbles on the local skin friction. Symbols: measurements of Madavan *et al.* [2]; $U^\infty = 10.7$ m/s \square ; 4.6 m/s ∇ ; \blacktriangledown is used for the probe located at 102 mm. Lines: predictions; ----- Batchelor viscosity model; ——— Einstein viscosity model.

out of the boundary layer still exists but is less pronounced than in the opposite case (plate below the boundary layer). Calculations were made by using: first, Einstein's viscosity model (curves 1 and 2) and second, Batchelor–Green's viscosity model (curve 3). The agreement between Einstein's model and the measurements is excellent. But since equation (29) is valid for a section located at the trailing edge of the injection area, such a good agreement requires special comments. As a matter of fact as one moves 51 mm downstream the probe location, one can observe in Fig. 3 that for a given concentration, the skin friction ratio increases significantly. This means that drag reduction is less important, due to the migration process aforementioned. From this physical argument, one can expect a decrease in the same proportion, if one moves 51 mm upstream. This tendency would involve that the experimental data be then better fitted by Batchelor–Green's formula than by Einstein's one. Henceforth, it is reasonable to think that microbubble interactions are to be taken into account in the modeling. The main problem is the choice of an adequate viscosity formulation. According to [4], Sibree's correlation is proven to work satisfactorily. The present study indicates that the Batchelor–Green model also provides acceptable predictions. In such conditions, more assertive conclusion could be drawn provided that measurements were performed at the immediate vicinity of the trailing edge of the injection section.

Finally, it is to be noted that over the parameter range investigated in Fig. 3, liquid velocity has very little influence on the drag reduction, which is confirmed by equation (29).

4. CONCLUDING REMARKS

The present work is an attempt to give a simple analytical formulation for microbubble drag reduction. This formulation is derived by assuming that the sublayer thickening is a highly probable mechanism in the reduction process. It leads to a model which is tested against the experimental data available in the literature. The predictions delivered by this model satisfactorily reproduce the trends and the order of magnitude of the measurements obtained close to the injection section. However a complete validation of the theory is not possible without a detailed experimental description of the corresponding boundary layers.

In particular, measurements of the velocity and of the gas concentration near the wall would be very useful to check the existence of a sublayer thickening and better analyse the influence of microbubble migration.

Acknowledgements—This research was sponsored by the DRET office (contract No 83/368).

NOMENCLATURE

C	constant in the logarithmic profile
CF	skin friction coefficient
K	wave number
0	index for single-phase flow
Q_{bubbles}	volumetric concentration of microbubbles per unit width of boundary layer
Q_{total}	total volumetric concentration (liquid and bubbles) per unit width of boundary layer
s	non-dimensional sublayer thickness
U	mean liquid velocity
U^{∞}	mean liquid velocity at the infinity
U^*	friction velocity
Y	distance from the wall
δ	boundary layer thickness
μ	molecular viscosity
ν	kinematic viscosity
$2\pi/\chi$	wake strength in the defect logarithmic profile
ρ	density
ϕ	bubble concentration in the boundary layer
ϕ_m	maximum bubble concentration in the boundary layer
χ	Von Karman's constant
$()_0^+$	non-dimensionalisation by U^* and ν_0 .

REFERENCES

1. J. L. Lumley, Drag reduction in two phase and polymer flows. *Physics Fluids* **20**(10), S64–S71 (1977).
2. N. K. Madavan, S. Deutsch and C. L. Merkle, Measurements of local skin friction in a microbubble-modified turbulent boundary layer. *J. Fluid Mech.* **156**, 237–256 (1985).
3. H. H. Legner, A simple model for gas bubble drag reduction. *Physics Fluids* **27**, 2788–2790 (1984).
4. N. K. Madavan, C. L. Merkle and S. Deutsch, Numerical investigations into the mechanisms of microbubble drag reduction. *J. Fluids Engng* **107**, 370–377 (1985).
5. J. O. Sibree, The viscosity of froth. *Trans. Faraday Soc.* **30**, Part II, 325–331 (1934).
6. V. G. Bogdevich, A. R. Evseev, A. G. Malyuga and G. S. Migirenko, Gas-saturation effect on near-wall turbulence characteristics. 2nd Int. Conference on Drag Reduction, Cambridge U.K., BHRA Fluid Engng, paper D2, 25–37 (1977).
7. J. L. Lumley, Drag reduction in turbulent flow by polymer additives. *J. Polymer Sci.: Macromol. Rev.* **7**, 263–290 (1973).
8. N. K. Madavan, S. Deutsch and C. L. Merkle, Reduction of turbulent skin friction by microbubbles. *Physics Fluids* **27**(2), 356–363 (1984).
9. J. L. Marié, A modelling of the skin friction and heat transfer in turbulent two-component bubbly flows in pipes. *Int. J. of Multiphase Flow*. To be published.
10. J. L. Lumley, Drag reduction by additives. *Ann. Rev. Fluid Mech.* **1**, 367–384 (1969).
11. H. Tennekes and J. L. Lumley, *A First Course in Turbulence*. M.I.T. Press, Cambridge, MA (1972).
12. M. S. Kolansky, S. Weinbaum and R. Pfeffer, Drag reduction in dilute gas–solid suspension flow: gas and particle velocity profiles. 3rd Int. Conference on the Pneumatic Transport of Solids in Pipes, BHRA Fluid Engng, paper C1, 1–19 (1976).
13. D. Coles, The law of the wake in turbulent boundary layer. *J. Fluid Mech.* **1**, 191–226 (1956).
14. R. Pfeffer and R. S. Kane, A review of drag reduction in dilute gas–solids suspension flow in tubes. 1st Int. Conference on Drag Reduction, Cambridge U.K., BHRA Fluid Engng, paper D5, 57–68 (1974).
15. A. Einstein, Eine neue Bestimmung der Moleküldimensionen. *Ann. Phys.* **19**, 289 (1906); **34**, 591 (1911).
16. G. K. Batchelor and J. T. Green, The determination of the bulk stress in a suspension of spherical particles to order C^2 . *J. Fluid Mech.* **56**, 401–427 (1972).
17. G. K. Batchelor, The effect of Brownian motion on the bulk stress in a suspension of spherical particles. *J. Fluid Mech.* **83**, 97–117 (1977).
18. H. Schlichting, *Boundary Layer Theory*. McGraw Hill, New York (1960).